

Tricellulin Modulates Transport of Macromolecules in the Salivary Gland

Journal of Dental Research
2020, Vol. 99(3) 302–310
© International & American Associations
for Dental Research 2019
Article reuse guidelines:
sagepub.com/journals-permissions
DOI: 10.1177/0022034519896749
journals.sagepub.com/home/jdr

S.N. Min^{1*}, X. Cong^{2*} , Y. Zhang², R.L. Xiang², Y. Zhou³, G.Y. Yu¹,
and L.L. Wu²

Abstract

Volume and composition of saliva are crucial for oral and systemic health. How substances, particularly macromolecules, are transported across the salivary gland epithelium has not been established in detail. Tricellulin is a component of tricellular tight junctions that form a central tube to serve as an important route for macromolecule transport. Whether tricellulin is expressed in the submandibular gland (SMG) and involved in salivation has been unknown. Here, by using Western blotting and immunofluorescence, tricellulin was found to be characteristically localized at tricellular contacts of human, rat, and mouse SMGs. Knockdown of tricellulin significantly increased, whereas overexpression of tricellulin decreased, paracellular permeability for 40-kDa but not for 4-kDa fluorescein isothiocyanate–dextran, while transepithelial electrical resistance was unaffected. Conversely, claudin-4 knockdown and overexpression affected transepithelial electrical resistance but not 40-kDa fluorescein isothiocyanate–dextran transport, suggesting that tricellulin regulated transport of macromolecules but not ions, which were mainly regulated by bicellular tight junctions (bTJs). Moreover, tricellulin was dynamically redistributed from tri- to bicellular membranes in cholinergically stimulated SMG tissues and cells. Immunoglobulin-like domain-containing receptor 1 (ILDR1) recruits tricellulin to tricellular contacts. The proportion of macromolecules in the saliva was increased, whereas the amount of stimulated saliva was unchanged in *Ildr1*^{-/-} mice, which displayed abnormal tricellulin distribution in SMGs. Furthermore, tricellulin interacted with bTJ proteins, such as occludin, claudin-1, claudin-3, claudin-4, and ZO-1, in rat SMG epithelial polarized cell line SMG-C6. Knockdown of tricellulin decreased occludin levels. Thus, we revealed a specific expression pattern of tricellulin in SMG epithelium. Tricellulin not only functioned as a barrier for macromolecules but also modulated the connection of bTJs to the tight junction complex. Alterations in tricellulin expression and distribution could thereby change salivary composition. Our study provided novel insights on salivary gland tight junction organization and function.

Keywords: tight junction, submandibular gland, secretion, occludin, claudin, angulin

Introduction

Saliva is important for maintaining oral homeostasis, including chewing, tasting, and swallowing functions and mechanical clearance with antimicrobial properties, which help defend the mucosa from infection (Carpenter 2013). Saliva is a heterogeneous biofluid containing water, inorganic ions, and organic components, such as enzymes, antibodies, hormones, lipids, and lysozymes. Under pathologic conditions, not only is the volume of saliva changed, but the composition can also be altered, which affects the oral cavity and overall health. In the saliva obtained from patients with Sjögren's syndrome, the levels of autoantibodies, inflammatory factors, and other proteins are significantly elevated (Katsiogiannis and Wong 2016; Kaczor-Urbanowicz et al. 2017). Exploring the secretory process of macromolecules under physiologic and pathologic conditions will help us understand the mechanism of salivary secretion and uncover the potential of saliva as a valuable non-invasive diagnostic tool in oral and systemic diseases.

The transport of substances across the salivary gland epithelium is mediated by 2 major pathways: the pore-based transepithelial pathway and the tight junction (TJ)–regulated paracellular pathway. TJs at the most apicolateral portion

between neighboring cells act as a barrier to the passage of water, ions, and multiple molecules (Tsukita et al. 2001; Furuse 2010). Tricellulin is a tetraspan tricellular TJ (tTJ) protein

¹Department of Oral and Maxillofacial Surgery, Peking University School and Hospital of Stomatology, National Engineering Laboratory for Digital and Material Technology of Stomatology, Beijing, China

²Department of Physiology and Pathophysiology, Peking University School of Basic Medical Sciences, Key Laboratory of Molecular Cardiovascular Sciences, Ministry of Education, and Beijing Key Laboratory of Cardiovascular Receptors Research, Beijing, China

³Department of Clinical Laboratory, China-Japan Friendship Hospital, Beijing, China

*Authors contributing equally to this article.

A supplemental appendix to this article is available online.

Corresponding Authors:

G.Y. Yu, Department of Oral and Maxillofacial Surgery, Peking University School and Hospital of Stomatology, 22 Zhong Guan Cun South St., Beijing, 100081, China.

Email: gyyu@263.net

L.L. Wu, Department of Physiology and Pathophysiology, Peking University School of Basic Medical Sciences, No. 38 Xueyuan Road, Haidian District, Beijing, 100191, China.

Email: pathophy@bjmu.edu.cn

discovered in 2005 (Ikenouchi et al. 2005). In contrast to the known transmembrane TJ proteins, such as claudins and occludin, which are widely expressed at membranes between 2 neighboring cells and so-called bicellular TJs (bTJs), tricellulin is principally concentrated at tricellular contacts (Krug et al. 2009). Subsequently, the angulin family members, including angulin-1/lipolysis-stimulated lipoprotein receptor, angulin-2/immunoglobulin-like domain-containing receptor 1 (ILDR1), and angulin-3/ILDR2, have been identified as tTJ-associated proteins that recruit tricellulin to tricellular contacts (Masuda et al. 2011; Higashi et al. 2013; Higashi et al. 2015). To date, tricellulin has been found in diverse epithelial tissues, including testis, small intestine, kidney, lung, and liver, as well as in epithelial cell lines, including intestinal HT-29/B6, Caco-2, and T84; kidney MDCK I, MDCK II, and M-1; and mammary Eph4 (Ikenouchi et al. 2005; Krug et al. 2009).

We previously found that secretagogues, such as muscarinic acetylcholine receptor (mAChR) agonists (e.g., carbachol, cevimeline, and pilocarpine) and the transient receptor potential vanilloid 1 agonist capsaicin, promote salivation by regulating TJ expression and/or distribution and by increasing paracellular permeability in submandibular glands (SMGs) (Cong et al. 2012; Cong et al. 2013; Cong et al. 2015; Li et al. 2015). Moreover, hyposalivatory SMGs from patients with Sjögren's syndrome and animal models are characterized by abnormal TJ expression and distribution with disrupted barrier function (Ewert et al. 2010; Mei et al. 2015; Zhang et al. 2016). These data suggest that TJs are dynamically altered in parallel with the secretion amount, but their contribution to the transport of molecules of different size has remained undetermined.

It has been found that bTJs mainly regulate permeability to ions and midsize solutes (molecular mass [M_r], 0.4 kDa), whereas in contrast, tricellulin at tTJs forms a barrier to macromolecules (M_r , 4 and 10 kDa) without affecting ions in tricellulin-overexpressing MDCK II cells (Krug et al. 2009). Furthermore, mutations in the *MARVELD2* gene encoding tricellulin cause nonsyndromic familial deafness in human (DFNB49) and hearing loss in mouse due to disrupted barrier function of the inner ear epithelium (Riazuddin et al. 2006; Nayak et al. 2013). Notably, mice with mutations in *Marveld2* gene show histologic abnormalities in multiple tissues, including the salivary gland. However, whether tricellulin is expressed in the salivary gland and how it regulates the paracellular transport of substances is still unknown.

Therefore, we sought to examine tricellulin expression in SMG tissues and cells. By using overexpression and knock-down techniques, we explored a possible role of tricellulin in the regulation of ion and macromolecule transport in SMGs. Furthermore, we investigated how the expression and distribution of tricellulin was affected by mAChR activation and the knockout of *Ildr1* gene.

Materials and Methods

Reagents and Antibodies

Pilocarpine, carbachol, fluorescein isothiocyanate (FITC)-labeled dextran (M_r , 4 and 40 kDa), and cell culture constituents were purchased from Sigma-Aldrich. Antibodies against

tricellulin, occludin, and ZO-1 were from Life Technologies. Antibodies against claudin-1, claudin-3, and claudin-4 were from Bioworld Technology.

Cell Culture

Rat SMG epithelial polarized cell line SMG-C6 (a gift from Prof. David O. Quissell) was cultured at 37 °C with 5% CO₂ in DMEM/F12 containing the following: 2.5% fetal bovine serum; 5 mg/L, transferrin; 1.1 μmol/L, hydrocortisone; 0.1 μmol/L, retinoic acid; 2 nmol/L, thyronine T3; 5 mg/L, insulin; 80 μg/L, epidermal growth factor; 50 mg/L, gentamicin sulfate; 5 mol/L, glutamine; 100 U/mL, penicillin; and 100 mg/L, streptomycin. Human embryonic kidney cell line 293T was purchased from the American Type Culture Collection (ATCC CRL-3216) and cultured in DMEM supplemented with 10% fetal bovine serum. Cells were also transfected with cDNA or shRNA plasmids for tricellulin, claudin-4, and occludin synthesized by OriGene Technologies and by using MegaTran 1.0 according to the manufacturer's instructions.

Human SMG Tissue Collection

Human SMG tissues were collected from the patients who underwent functional neck dissection for primary oral squamous cell carcinoma without irradiation or chemotherapy. The tissues were confirmed to be histologically normal and used as controls. The research was approved by the Ethics Committees for Human Experiments of Peking University School and Hospital of Stomatology (No. PKUSSIRB-2013008). All patients signed an informed consent document before tissue collection.

Saliva Secretion Measurements

C57BL/6 male mice (8 to 10 wk old) were obtained from the Peking University Health Science Center. *Ildr1*^{-/-} mice were a gift from Prof. Lei Wang and Prof. Zhi-Gang Xu (Sang et al. 2015). The primers used for genotyping are shown in Appendix Table 1. For the detailed measurement process, refer to the Appendix Methods. All experimental procedures were approved by the Ethics Committee of Animal Research of the Peking University Health Science Center (No. LA2017138) and complied with the *Guide for the Care and Use of Laboratory Animals* (National Institutes of Health publication 85-23, revised 1996). All animal research is reported in accordance with the ARRIVE guidelines (Kilkenny et al. 2010).

Detection of Proteins and Electrolytes in Serum and Saliva

After saliva and serum were collected, the proteins were detected by capillary electrophoresis (Capillary2 Flex Piercing; Sebia). For the detailed capillary electrophoresis detection, refer to the Appendix Methods. We also stained proteins in SDS-PAGE gels with Coomassie blue, which allows visualization of proteins as blue bands on a clear background. Moreover, serum and saliva concentrations of electrolytes, as

well as serum content of albumin (M_r , ~67 kDa), which is a typical paracellular component, were measured by the Beckman Coulter Chemistry Analyzer AU5800 series.

Transepithelial Electrical Resistance Measurements

SMG-C6 cells were seeded at a low density (1×10^4 cells/cm²) in Costar 24-well Transwell chambers (filter pore size, 0.4 μ m; filter area, 0.33 cm²). Transepithelial electrical resistance (TER) was measured at 37 °C with an epithelial volt/ohm meter EVOM2 (World Precision Instruments). Cells were gradually grown to form a confluent monolayer for 5 to 7 d. When TJ barrier integrity was well established among cells, the TER value would reach a platform to gain maximal values and be ready for experiments. The TER value ($\Omega \cdot \text{cm}^2$) was calculated by subtracting the blank filter (90 Ω) and by multiplying the filter area.

Paracellular Permeability Assay

FITC-dextran (1 g/L) was added into the lower chamber of SMG-C6 monolayers for 3 h; the apical solution was collected; and fluorescent intensity was determined by an EnSpire Multilabel Plate Reader (PerkinElmer). The apparent permeability coefficient (Papp) value was determined as the increase in the amount of tracer per time per filter area (Cong et al. 2015).

Statistical Analysis

Data are shown as the mean \pm SEM. Statistical analysis was performed by Student's *t* test between 2 groups. $P < 0.05$ was considered statistically significant.

For human SMG tissue stimulation, saliva secretion measurements, capillary electrophoresis, Western blotting, separation of membrane and cytoplasm fractions, immunofluorescence, enzyme-linked immunosorbent assay, real-time polymerase chain reaction, and coimmunoprecipitation, refer to the Appendix.

Results

Expression of Tricellulin in SMG Tissues and Cells

Tricellulin expression in SMG was revealed by Western blotting as multiple bands in the M_r range of 66 to 72 kDa. Proteins from rat intestine and mouse kidney tissues served as positive controls. Intriguingly, bands with lower M_r were predominant in rat, human, and mouse SMG tissues, whereas in SMG-C6 cells, the band with higher M_r was predominant (Fig. 1A). By separating the cytoplasm and membrane fractions of SMG-C6 cells, we showed that tricellulin was mostly displayed within the membrane fraction (Fig. 1B). Cell surface biotinylation assay showed predominant tricellulin expression in the biotinylated cell membrane fraction (Fig. 1C). After treatment with calf intestinal phosphatase, the higher M_r band from SMG-C6 cells migrated into the lower level, similar to that observed in

human SMG tissues (Fig. 1D), suggesting a highly phosphorylated state of tricellulin in SMG-C6 cells.

Concentration of Tricellulin at Tricellular Contacts in SMGs

In control human and mouse SMG tissues, tricellulin was expressed in the acini and ducts, presenting mainly as dots and short rods at the most apical portion of lateral membranes (arrowheads in Fig. 1E). In contrast, ZO-1 and occludin exhibited prolonged positive lines along lateral membranes at bicellular contacts (Fig. 1F). An illustration showing the position of tTJs and bTJs is shown in Figure 1G. In SMG-C6 cells, tricellulin dot-like expression was principally localized to tricellular contacts in 2- and 3-dimensional images (Fig. 2A, upper and middle panels). Tricellulin was found at a similar depth as claudin-1 along the lateral membranes (Fig. 2A, lower panel). Moreover, coimmunofluorescence images showed a typical spider web-like distribution of bTJs (occludin and claudin-4), with dots of tricellulin in points of contact among 3 cells (Fig. 2B). These data suggest that tricellulin is characteristically expressed at tricellular contacts in SMG tissues and cells. By contrast, in 293T cells, which do not express TJs and have no polarization, transfected tricellulin was widely expressed at bi- and tricellular membranes (Appendix Fig. 1).

Regulation of Macromolecule Paracellular Transport in SMGs by Tricellulin

To explore its role in paracellular permeability, we knocked down and overexpressed tricellulin in SMG-C6 cells. Interestingly, knockdown of tricellulin significantly increased, whereas overexpression of tricellulin reduced the Papp values of 40-kDa FITC-dextran; however, neither knockdown nor overexpression of tricellulin affected the TER values or permeation of 4-kDa FITC-dextran (Fig. 2C, D). In contrast, knockdown or overexpression of claudin-4 significantly decreased or increased the TER values without affecting the Papp values, suggesting a functional difference between tricellulin and claudin-4 in the regulation of paracellular transport.

Redistribution of Tricellulin upon mAChR Activation

To investigate the involvement of tricellulin in salivation, we next examined the effect of mAChR activation on tricellulin distribution and expression. In cultured human SMG tissues, stimulation with 10- μ mol/L carbachol for 5 min caused tricellulin redistribution from the most apicolateral dot-like concentrating portions to lateral membranes at bicellular contacts (arrowheads in Fig. 3A). Similar phenomenon was seen in mouse SMGs after injection of pilocarpine (arrowheads in Fig. 3B). In SMG-C6 cells, carbachol treatment significantly induced tricellulin redistribution from tricellular contacts to bicellular interactions (Fig. 3C). Furthermore, tricellulin levels in total protein homogenates were unchanged by carbachol in SMG-C6 cells and tricellulin-transfected 293T cells (Fig. 3D).

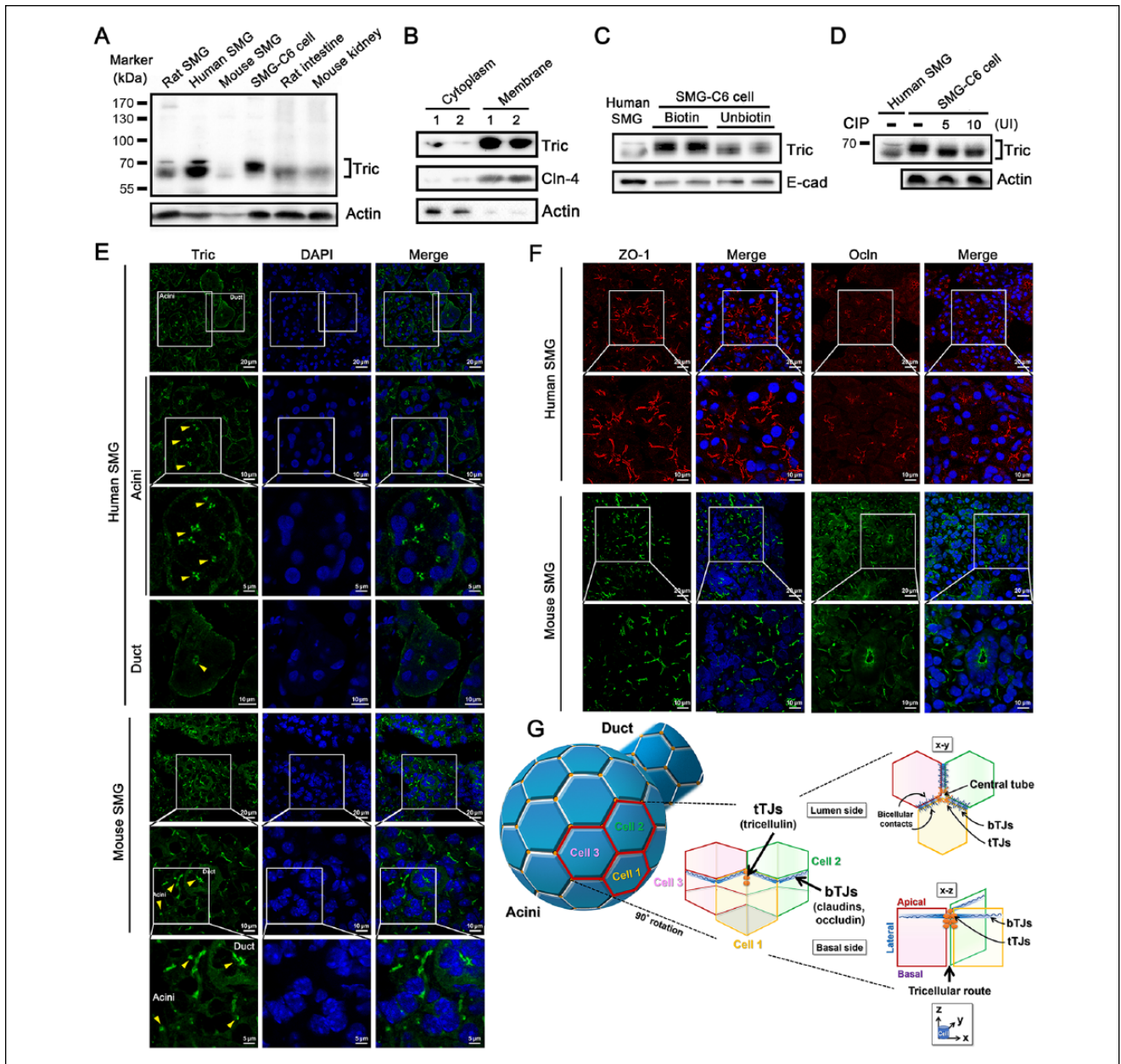


Figure 1. Expression pattern of tricellulin in submandibular gland (SMG) tissues and cells. **(A)** Tricellulin expression in rat, human, and mouse SMG tissues, as well as SMG-C6 cells. Proteins extracted from rat intestine and mouse kidney served as positive controls. Tricellulin expression in the cytoplasm and cell membrane fractions was prepared from SMG-C6 cells by using a Nucl-Cyto-Mem Preparation Kit **(B)** or a Pierce Cell Surface Protein Isolation Kit **(C)**, respectively. **(D)** Tricellulin bands from SMG-C6 cells obtained after treatment with calf intestinal phosphatase (CIP; 5 and 10 UI). Proteins from human SMG tissues served as positive control. **(E)** Tricellulin localization in human and mouse SMG tissues. The enlarged images show acini and ducts (bars: 10 μm or 5 μm) derived from the boxes in the upper panels (bars: 20 μm). Arrowheads point to the specific dots and rods of tricellulin staining. **(F)** ZO-1 and occludin localization in human and mouse SMG tissues. The enlarged images (bars: 10 μm) derived from the boxes in the upper panels (bars: 20 μm). Cln, claudin; E-cad, E-cadherin; Ocn, occludin; Tric, tricellulin. **(G)** An illustration shows the spatial localization of tricellular tight junctions (tTJs) and bicellular tight junction (bTJs) in the acini of SMGs.

Enhanced Macromolecule Secretion in *Ildr1*^{-/-} Mice

Angulins are known to recruit tricellulin to tricellular contacts (Masuda et al. 2011; Higashi et al. 2013; Higashi et al. 2015). We therefore explored how targeted disruption of *Ildr1*, which encodes angulin-2/ILDR1 in mice, affected tricellulin function

and salivation in SMGs (Fig. 4A). No significant differences in body weight, SMG weight, or saliva amount were found between *Ildr1*^{+/+} and *Ildr1*^{-/-} mice (Fig. 4B, C). *Ildr1*^{-/-} mice did not show any apparent histological abnormality in SMGs (Fig. 4D). However, tricellulin was redistributed from tricellular contacts to more prolonged bicellular junctions, whereas

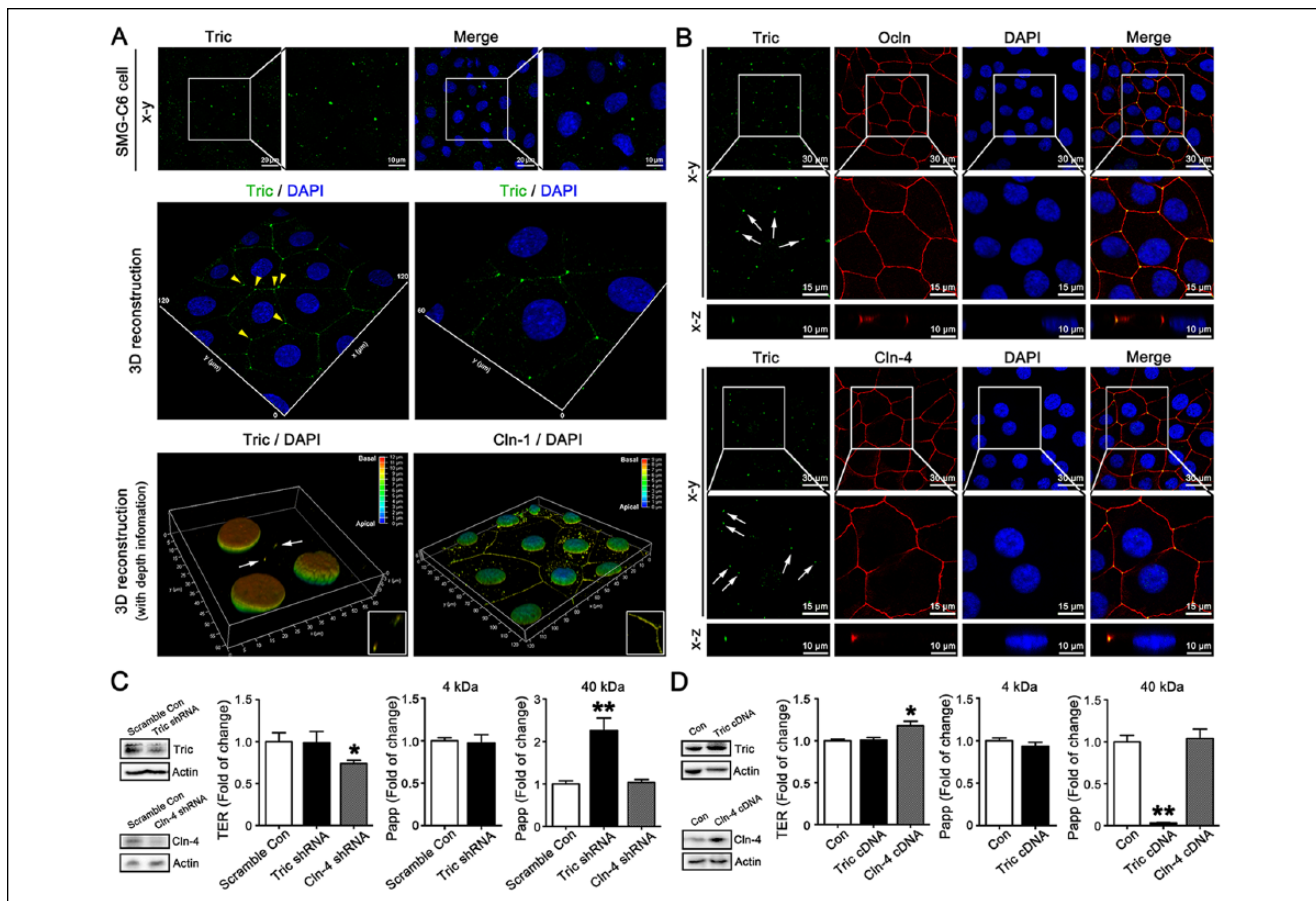


Figure 2. Distribution and function of tricellulin in SMG-C6 cells. **(A)** Immunofluorescence images show tricellulin localization in the x-y plane (top), 3-dimensional (3D) reconstruction (middle), and 3D images with the depth information (bottom). Arrowheads and arrows point to specific dots of tricellulin staining. In 3D images with the depth information, the height labeling from the apical (blue) to basal (red) sides of cells is shown at the top right, and the enlarged images show tricellulin and claudin-1 within white boxes at the bottom right. **(B)** Coimmunofluorescence images show the localization of tricellulin with occludin and claudin-4 in both x-y and x-z planes. The enlarged x-y images (bars: 15 μ m) were derived from boxes in the upper panels (bars: 30 μ m). Arrows indicate the specific dots of tricellulin staining. **(C)** The effect of tricellulin and claudin-4 downregulation on the transepithelial electrical resistance (TER) and apparent permeability coefficient (Papp) values in SMG-C6 cells. TER value was measured by using EVOM2, whereas the Papp value was calculated in the paracellular permeability assay by using 4- and 40-kDa FTIC-dextran as paracellular tracers. **(D)** The effect of tricellulin and claudin-4 overexpression on TER and Papp values for 4- and 40-kDa FTIC-dextran in SMG-C6 cells. All data are presented as the means \pm SEM of results from 6 independent experiments. * $P < 0.05$ and ** $P < 0.01$ as compared with controls. Cln, claudin; Con, control; Ocln, occludin; Tric, tricellulin.

claudin-1 intensity was enhanced at plasma membranes in the acini of *Ildr1*^{-/-} mice (Fig. 4E). In SMGs, tricellulin and occludin mRNA levels were unchanged, whereas claudin-1, claudin-3, claudin-4, and ZO-1 mRNA levels were significantly increased in *Ildr1*^{-/-} as compared with those in *Ildr1*^{+/-} mice (Fig. 4F).

To explore the role of tricellulin in SMGs of *Ildr1*^{-/-} mice, we examined salivary composition. Capillary electrophoresis detection experiments did not reveal any significant change in the proportions of serum proteins with different *Mr* between *Ildr1*^{+/-} and *Ildr1*^{-/-} mice (Fig. 4G). By contrast, in pooled saliva, slight decreases in low *Mr* parts (parts 1 to 3) and an increase in the middle *Mr* part (part 4) in *Ildr1*^{-/-} mice were observed, whereas the fraction of large *Mr* proteins (part 5) was not altered (Fig. 4H). We also performed Coomassie blue staining to visualize protein bands. Fractions of proteins with *Mr* between 50 and 95 kDa were higher in saliva of

Ildr1^{-/-} mice than in *Ildr1*^{+/-} mice (arrows in Fig. 4I), although this phenomenon was not observed in serum protein gels. Furthermore, saliva albumin levels were higher in *Ildr1*^{-/-} mice than in *Ildr1*^{+/-} mice, whereas serum albumin levels were similar (Fig. 4J). Serum and saliva concentrations of electrolytes, including Na⁺, Cl⁻, Ca²⁺, inorganic phosphorus, and K⁺, were similar between *Ildr1*^{+/-} and *Ildr1*^{-/-} mice, whereas Mg²⁺ concentration was significantly lower in serum but not in saliva of *Ildr1*^{-/-} mice (Appendix Fig. 2).

Interaction of Tricellulin with bTJs and ZO-1 in SMGs

To fully evaluate the role of tricellulin in SMG epithelium, we further explored the interactions between tricellulin and bTJs and ZO-1. Tricellulin coimmunoprecipitated with occludin, claudin-1, claudin-3, claudin-4, and ZO-1 in SMG-C6 cells (Fig. 5A, B). Because tricellulin shares sequence homology

with occludin, especially in the region of ~130 highly conserved C-terminal amino acids (Raleigh et al. 2010), the relationship between these proteins was particularly examined. Knockdown of tricellulin significantly decreased occludin expression, whereas overexpression of tricellulin did not affect occludin levels in SMG-C6 cells (Fig. 5C–F), suggesting that tricellulin loss influenced bTJ expression levels. Conversely, neither knock-down nor overexpression of occludin influenced tricellulin expression (Fig. 5G–J).

Discussion

In the present study, we demonstrated characteristic localization of tricellulin at tricellular contacts in SMG tissues and cells. Moreover, we confirmed that tricellulin played an important role in regulating paracellular transport of macromolecules in salivary epithelium. Activation of mAChR induced dynamic tricellulin redistribution from tricellular contacts to bicellular junctions. In SMGs of *Ildr1^{-/-}* mice, tricellulin was mislocated to lateral membranes, and the transport of macromolecules, but not ions or small-sized molecules, was enhanced. As an integral part of the TJ complex, tricellulin interacts with bTJs, so alterations in its expression and distribution affected the expression of bTJs in SMGs.

Although tTJ ultrastructure has been observed by electron microscopy for more than 50 y, its protein composition was unclear until tricellulin was discovered during gene screening in 2005 (Staelin et al. 1969; Walker et al. 1985; Ikenouchi et al. 2005). Nowadays, it is well accepted that bTJs are zipper-like structures that seal bicellular spaces but end at tricellular corners, where tTJs are vertically localized (Higashi and Miller 2017). To seal the tricellular space, tTJs form a very long and narrow specialized tubular structure (~10 nm in diameter) that serves as a strict barrier (Mariano et al. 2011; Furuse et al. 2014). Tricellulin has been observed in various epithelia and endothelia, but whether it was expressed in salivary glands has been unknown. Here, we showed tricellulin expression in rat, human, and mouse SMG tissues with a *Mr* range similar to the previous study in mouse epithelial cell lines Eph4, CSG1, and MTD1A (Ikenouchi et al. 2005). Tricellulin was principally distributed at apicolateral membranes and displayed as dots and rods toward the lumen in the acini and ducts of SMG tissues. In SMG-C6 cells, staining for tricellulin had a characteristic dot-like pattern concentrated at tricellular corners.

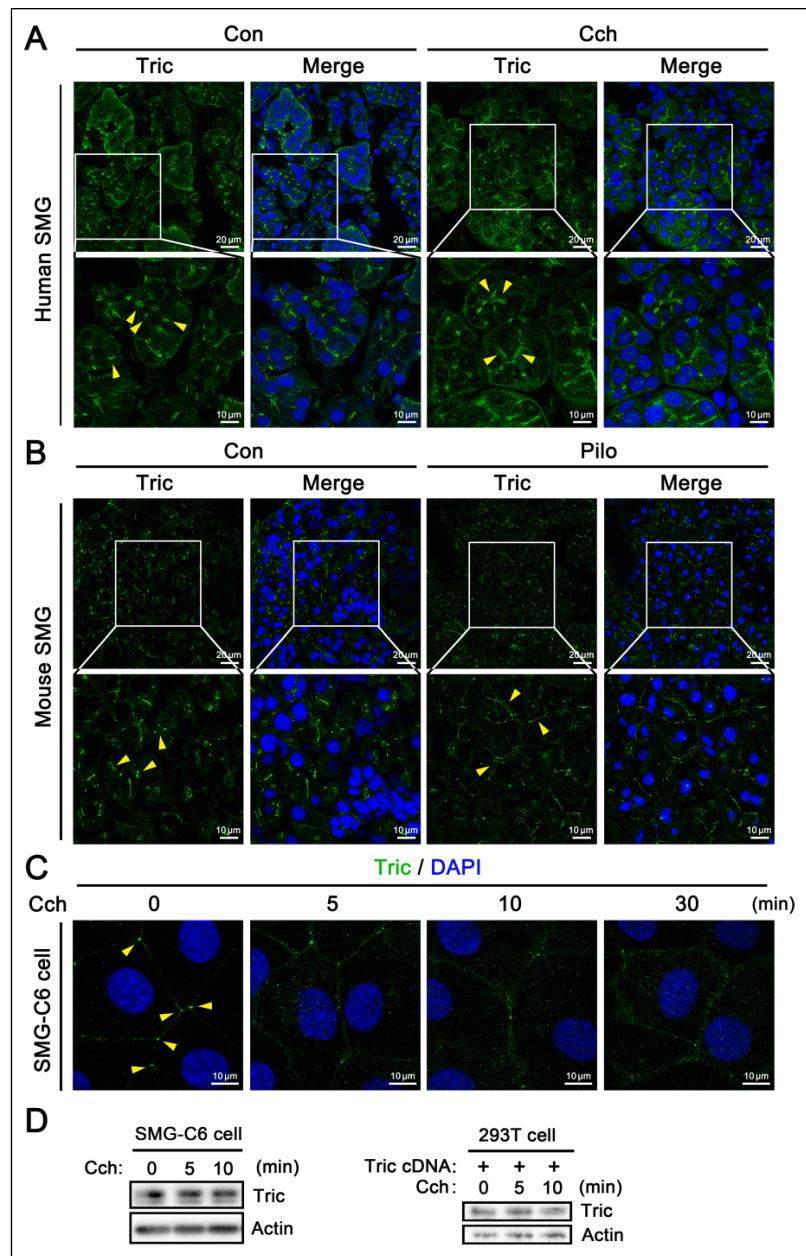


Figure 3. Alteration of tricellulin distribution by the activation of the muscarinic acetylcholine receptor (mAChR) in submandibular gland (SMG) tissues and cells. **(A)** Human SMG tissues were incubated with 10 μ mol/L of carbachol for 5 min, and the distribution of tricellulin staining was examined. Arrowheads point to tricellulin staining. Bars: 20 and 10 μ m. **(B)** SMGs were harvested from control and pilocarpine-stimulated mice, and immunofluorescence images of tricellulin were taken. Arrowheads point to tricellulin staining. Bars: 20 and 10 μ m. **(C)** SMG-C6 cells were treated with carbachol for 5, 10, and 30 min, and the changes of tricellulin distribution were captured by confocal microscopy. Bars: 10 μ m. **(D)** The effect of carbachol stimulation for 5 and 10 min on tricellulin protein levels in SMG-C6 and 293T cells pretransfected with tricellulin cDNA. Cch, carbachol; Con, control; Pilo, pilocarpine; Tric, tricellulin.

TER measurement and paracellular permeability assay—2 routine methods to evaluate TJ barrier function—gauge ionic conductance of the paracellular pathway and mainly paracellular transport of noncharged macromolecules, respectively. In Eph4 cells, tricellulin suppression by RNAi leads to reduced TER and increased paracellular permeability for 4-kDa

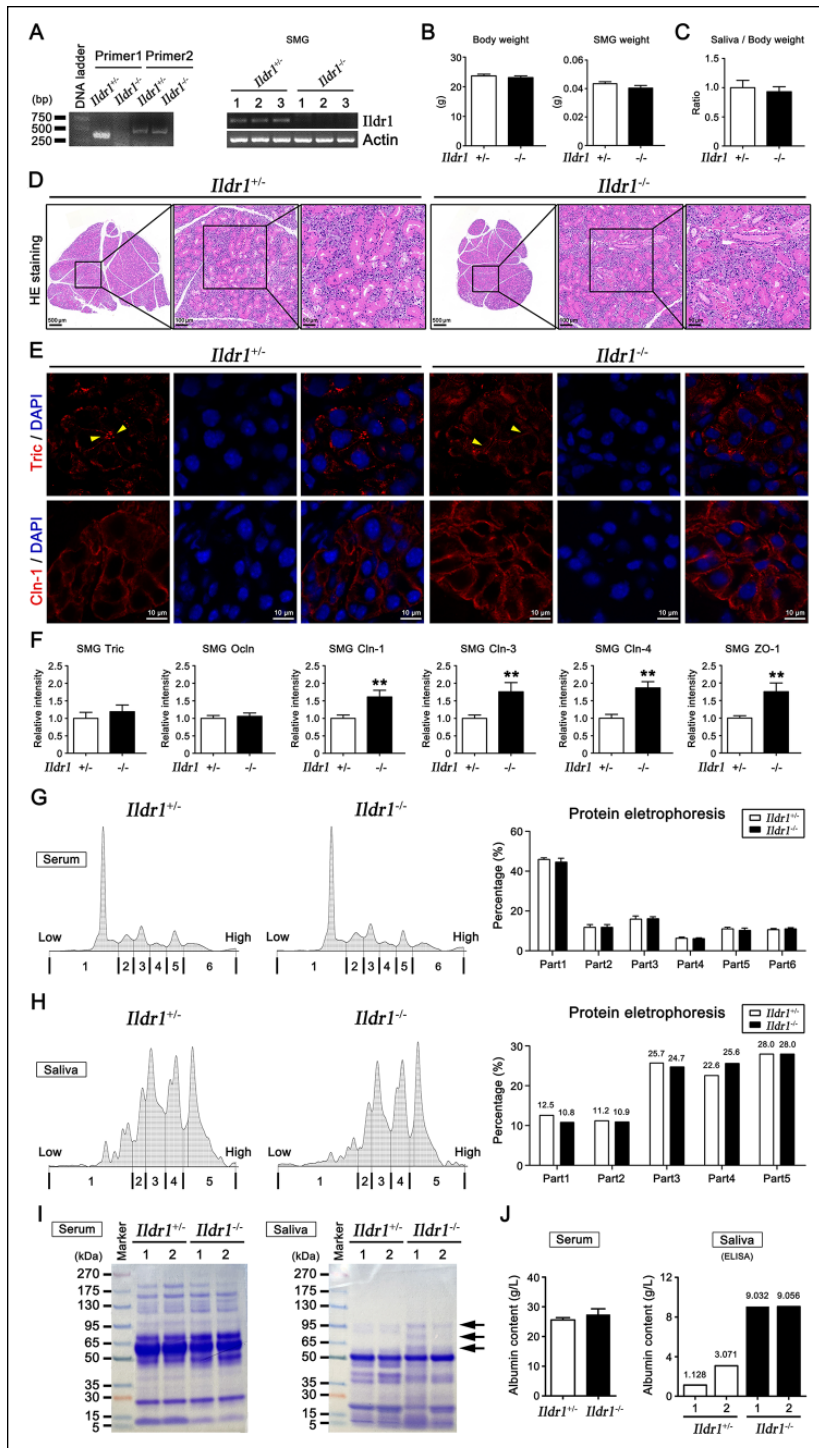


Figure 4. Pattern of secretion in mice with the knockout of immunoglobulin-like domain-containing receptor 1 (*Ildr1*) gene and tight junction expression in submandibular glands (SMGs). **(A)** Left: genotyping of *Ildr1*^{+/+} and *Ildr1*^{-/-} mice by 2 polymerase chain reaction primers. Primer1 was used to identify the wild-type allele (365-bp band), and primer2 was used to identify the knockout allele (514-bp band). Right: *Ildr1* mRNA bands (140 bp) in SMG tissues from *Ildr1*^{+/+} and *Ildr1*^{-/-} mice. **(B)** Body weight and SMG weight in *Ildr1*^{+/+} and *Ildr1*^{-/-} mice. **(C)** The ratio of the secreted saliva amount to body weight in *Ildr1*^{+/+} and *Ildr1*^{-/-} mice. **(D)** Histologic morphology of SMGs revealed by hematoxylin and eosin staining in *Ildr1*^{+/+} and *Ildr1*^{-/-} mice. The enlarged images derived from the black boxes. **(E)** Immunostaining for tricellulin and claudin-1 in SMG tissues of *Ildr1*^{+/+} and *Ildr1*^{-/-} mice. Arrowheads point to tricellulin-specific staining. **(F)** mRNA expression levels of tricellulin, occludin, claudin-1, claudin-3, claudin-4, and ZO-1 in SMG tissues of *Ildr1*^{+/+} and *Ildr1*^{-/-} mice. All data are presented

FITC-dextran, with abnormal localization of occludin around tricellular regions (Ikenouchi et al. 2005). In MDCK II cells, at low expression levels, tricellulin forms a pathway for macromolecules, whereas at high expression, it forms a barrier in tTJs for macromolecules and in bTJs for solutes of all sizes (Ikenouchi et al. 2008). In the inner ear epithelium, removal of tricellulin disrupts the structure of TJ strands and selectively affects paracellular permeability for ions and small molecules, resulting in a toxic microenvironment for cochlear hair cells. These data suggest that tricellulin plays an important role in TJ formation and paracellular barrier function, although permeation of macromolecules of different sizes and/or ions through the tricellulin-based “tube” varies in different tissues. In the present study, by using knockdown and overexpression approaches, we found that tricellulin acted as a barrier mainly against macromolecules with $M_r > 4$ kDa but not against ions. Therefore, tricellulin mainly regulates the transport of macromolecules through the tricellular pathway in SMGs.

The localization at tricellular contacts points to tricellulin barrier function. Poly-L-arginine, an absorption enhancer, enhances the paracellular permeability for hydrophilic macromolecules across the intestinal epithelium through the internalization of tricellulin and bTJs (Yamaki et al. 2013). Furthermore, tricellulin is a specific redox sensor that can be redistributed from tri- to bicellular contacts in response to ischemia, hypoxia, and reductants (Cording et al. 2015). Our present

as the means \pm SEM of results from 6 mice. $**P < 0.01$ as compared with *Ildr1*^{+/+} mice. Cln, claudin; Ocln, occludin; Tric, tricellulin. **(G)** Serum proteins from 5 *Ildr1*^{+/+} and *Ildr1*^{-/-} mice were separated by capillary electrophoresis. The representative curves are shown on the left. According to molecular weights and peaks, serum proteins were divided into 6 parts. The statistical analysis of the proportions of different parts is shown on the right. **(H)** Proteins of pooled saliva samples collected from 5 *Ildr1*^{+/+} or 5 *Ildr1*^{-/-} mice were separated by capillary electrophoresis. According to molecular weights and peaks, the saliva proteins were divided into 5 parts. The proportions of different parts of the saliva proteins with the numbers labeled on each column are shown on the right. **(I)** Serum and saliva proteins derived from *Ildr1*^{+/+} and *Ildr1*^{-/-} mice were stained with Coomassie blue in SDS-PAGE gels. Arrows point to the alteration of macromolecular bands in saliva. **(J)** Albumin levels in serum (6 mice per group) and saliva (2 mice per group) samples from *Ildr1*^{+/+} and *Ildr1*^{-/-} mice were detected by a Beckman Coulter Chemistry Analyzer and enzyme-linked immunosorbent assay (ELISA) method, respectively.

study showed that tricellulin localization was dynamically extended to bicellular contacts in SMGs by mAChR activation, which would allow the permeation of macromolecules into saliva. The involvement of tricellulin in pathologic processes, such as hearing loss, type 2 diabetes, bacterial pathogenesis, blood-brain and blood-retinal barrier disruption, and epithelial-to-mesenchymal transition, has been extensively investigated (Dokmanovic-Chouinard et al. 2008; Borck et al. 2011; Mariano et al. 2013; Nayak et al. 2013; Morozko et al. 2015; Morampudi et al. 2017). However, whether alterations of tricellulin affect salivation was still unknown. Here, we found that tricellulin was redistributed to lateral membranes at bicellular contacts in *Ildr1*^{-/-} mice and the proportion of macromolecules such as albumin was increased in secreted saliva, whereas saliva amount and concentrations of electrolytes were not altered, which suggested that tricellulin alteration changed saliva composition due to dysregulation of macromolecular secretion.

TJs comprise multiple proteins. Tricellulin interacts with claudins to form the TJ network, whereas whether tricellulin binds to ZO-1 and occludin remains debatable (Riazuddin et al. 2006). Our results showed that tricellulin interacted with bTJs and ZO-1 in SMG-C6 cells and that decreased protein expression of tricellulin affected occludin levels. However, the protein levels of occludin did not influence tricellulin expression. Moreover, loss of tricellulin at tricellular contacts in SMGs of *Ildr1*^{-/-} mice upregulated claudin levels. These data suggested that the interaction between tricellulin and bTJs was crucial to the establishment of the TJ complex and that alterations in tricellulin expression and/or distribution likely change bTJ characteristics.

In summary, we demonstrated for the first time that tricellulin was characteristically expressed at tricellular contacts in SMG, where it contributed to the paracellular transport of macromolecules. Furthermore, the interaction between tricellulin and bTJs indicated an important role of tricellulin in the formation of the TJ complex. Our findings provide novel insights into the involvement and significance of tricellulin in SMG.

Author Contributions

S.N. Min, X. Cong, contributed to data acquisition, analysis, and interpretation, drafted and critically revised the manuscript; Y. Zhang, R.L. Xiang, contributed to data analysis

and interpretation, critically revised the manuscript; Y. Zhou, contributed to data acquisition, drafted the manuscript; G.Y. Yu, L.L.

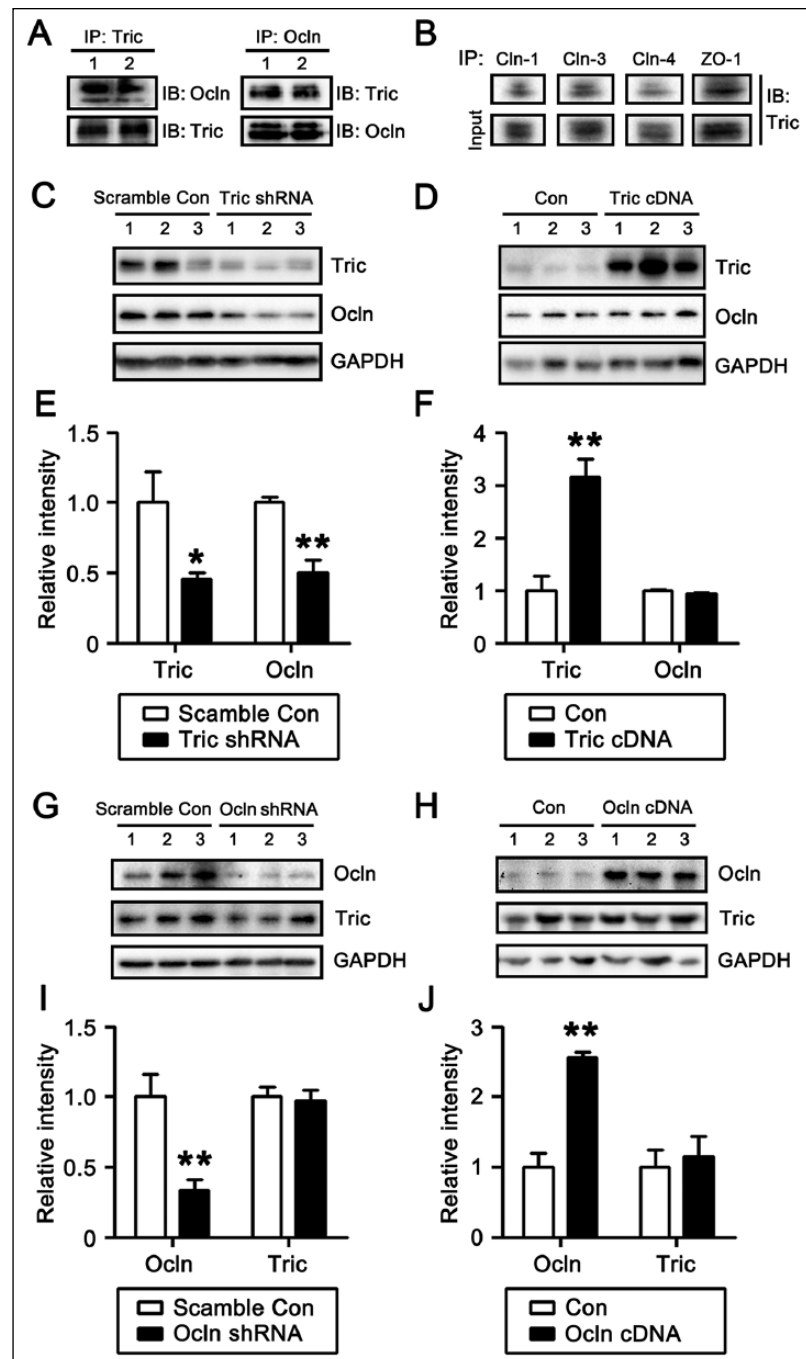


Figure 5. Interaction between tricellulin and bicellular tight junctions and ZO-1 in SMG-C6 cells. Interaction between tricellulin and occludin (A) and claudin-1, claudin-3, claudin-4, and ZO-1 (B) as detected by coimmunoprecipitation. IB, immunoblotting; IP, immunoprecipitation. Tricellulin and occludin protein expression levels following knockdown (C) and overexpression (D) of tricellulin. (E, F) The semiquantification on the protein band intensities shown in the above images. Tricellulin and occludin protein expression levels following knockdown (G) and overexpression (H) of occludin. (I, J) The semiquantification on the protein band intensities shown in the above images. All data are presented as the means \pm SEM of results from 6 independent experiments. * $P < 0.05$ and ** $P < 0.01$ compared with controls. Cln, claudin; Con, control; Ocln, occludin; Tric, tricellulin.

Wu, contributed to conception and design, critically revised the manuscript. All authors gave final approval and agree to be accountable for all aspects of the work.

Acknowledgments

We thank Dr. David O. Quissell from the School of Dentistry, University of Colorado Health Sciences Center, for the generous gift of the rat SMG-C6 cell line. We thank Prof. Lei Wang from the School of Life Sciences, Fudan University, and Prof. Zhi-Gang Xu from Shan Dong University for the generous gift of the *Ildr1*^{-/-} mouse model. We also thank Prof. Guo-He Zhang from the National Institute of Dental and Craniofacial Research, National Institutes of Health, for providing thoughtful suggestions. We would like to thank Editage (www.editage.com) for English language editing. This study was supported by the National Natural Science Foundation of China (grants 31972908 and 81771093). The authors declare no potential conflicts of interest with respect to the authorship and/or publication of this article.

ORCID iD

X. Cong  <https://orcid.org/0000-0001-5387-1414>

References

- Borck G, Ur Rehman A, Lee K, Pogoda HM, Kakar N, von Ameln S, Grillet N, Hildebrand MS, Ahmed ZM, Nürnberg G, et al. 2011. Loss-of-function mutations of ILDR1 cause autosomal-recessive hearing impairment DFNB42. *Am J Hum Genet.* 88(2):127–137.
- Carpenter GH. 2013. The secretion, components, and properties of saliva. *Annu Rev Food Sci Technol.* 4:267–276.
- Cong X, Zhang Y, Li J, Mei M, Ding C, Xiang RL, Zhang LW, Wang Y, Wu LL, Yu GY. 2015. Claudin-4 is required for modulation of paracellular permeability by muscarinic acetylcholine receptor in epithelial cells. *J Cell Sci.* 128(12):2271–2286.
- Cong X, Zhang Y, Shi L, Yang NY, Ding C, Li J, Ding QW, Su YC, Xiang RL, Wu LL, et al. 2012. Activation of transient receptor potential vanilloid subtype 1 increases expression and permeability of tight junction in normal and hyposcretory submandibular gland. *Lab Invest.* 92(5):753–768.
- Cong X, Zhang Y, Yang NY, Li J, Ding C, Ding QW, Su YC, Mei M, Guo XH, Wu LL, et al. 2013. Occludin is required for TRPV1-modulated paracellular permeability in the submandibular gland. *J Cell Sci.* 126(Pt 5):1109–1121.
- Cording J, Günther R, Vigolo E, Tscheik C, Winkler L, Schlattner I, Lorenz D, Haseloff RF, Schmidt-Ott KM, Wolburg H, et al. 2015. Redox regulation of cell contacts by tricellulin and occludin: redox-sensitive cysteine sites in tricellulin regulate both tri- and bicellular junctions in tissue barriers as shown in hypoxia and ischemia. *Antioxid Redox Signal.* 23(13):1035–1049.
- Dokmanovic-Chouinard M, Chung WK, Chevre JC, Watson E, Yanan J, Wiegand B, Bromberg Y, Wakae N, Wright CV, Overton J, et al. 2008. Positional cloning of “Lisch-like,” a candidate modifier of susceptibility to type 2 diabetes in mice. *PLoS Genet.* 4(7):e1000137.
- Ewert P, Aguilera S, Allende C, Kwon YJ, Albornoz A, Molina C, Urzúa U, Quest AF, Olea N, Pérez P, et al. 2010. Disruption of tight junction structure in salivary glands from Sjögren’s syndrome patients is linked to proinflammatory cytokine exposure. *Arthritis Rheum.* 62(5):1280–1289.
- Furuse M. 2010. Molecular basis of the core structure of tight junctions. *Cold Spring Harb Perspect Biol.* 2(1):a002907.
- Furuse M, Izumi Y, Oda Y, Higashi T, Iwamoto N. 2014. Molecular organization of tricellular tight junctions. *Tissue Barriers.* 2:e28960.
- Higashi T, Katsuno T, Kitajiri S, Furuse M. 2015. Deficiency of angulin-2/ILDR1, a tricellular tight junction-associated membrane protein, causes deafness with cochlear hair cell degeneration in mice. *PLoS One.* 10(3):e0120674.
- Higashi T, Miller AL. 2017. Tricellular junctions: how to build junctions at the TRICKiest points of epithelial cells. *Mol Biol Cell.* 28(15):2023–2034.
- Higashi T, Tokuda S, Kitajiri S, Masuda S, Nakamura H, Oda Y, Furuse M. 2013. Analysis of the “angulin” proteins LSR, ILDR1 and ILDR2-tricellulin recruitment, epithelial barrier function and implication in deafness pathogenesis. *J Cell Sci.* 126(Pt 4):966–977.
- Ikenouchi J, Furuse M, Furuse K, Sasaki H, Tsukita S, Tsukita S. 2005. Tricellulin constitutes a novel barrier at tricellular contacts of epithelial cells. *J Cell Biol.* 171(6):939–945.
- Ikenouchi J, Sasaki H, Tsukita S, Furuse M, Tsukita S. 2008. Loss of occludin affects tricellular localization of tricellulin. *Mol Biol Cell.* 19(11):4687–4693.
- Kaczor-Urbanowicz KE, Martin Carreras-Presas C, Aro K, Tu M, Garcia-Godoy F, Wong DT. 2017. Saliva diagnostics-current views and directions. *Exp Biol Med (Maywood).* 242(5):459–472.
- Katsiogiannis S, Wong DT. 2016. The proteomics of saliva in Sjögren’s syndrome. *Rheum Dis Clin North Am.* 42(3):449–456.
- Kilkenny C, Browne W, Cuthill IC, Emerson M, Altman DG. 2010. Animal research: reporting in vivo experiments: the ARRIVE guidelines. *Br J Pharmacol.* 160(7):1577–1579.
- Krug SM, Amasheh S, Richter JF, Milatz S, Günzel D, Westphal JK, Huber O, Schulzke JD, Fromm M. 2009. Tricellulin forms a barrier to macromolecules in tricellular tight junctions without affecting ion permeability. *Mol Biol Cell.* 20(16):3713–3724.
- Li J, Cong X, Zhang Y, Xiang RL, Mei M, Yang NY, Su YC, Choi S, Park K, Zhang LW, et al. 2015. ZO-1 and -2 are required for TRPV1-modulated paracellular permeability. *J Dent Res.* 94(12):1748–1756.
- Mariano C, Palmela I, Pereira P, Fernandes A, Falcão AS, Cardoso FL, Vaz AR, Campos AR, Gonçalves-Ferreira A, Kim KS, et al. 2013. Tricellulin expression in brain endothelial and neural cells. *Cell Tissue Res.* 351(3):397–407.
- Mariano C, Sasaki H, Brites D, Brito MA. 2011. A look at tricellulin and its role in tight junction formation and maintenance. *Eur J Cell Biol.* 90(10):787–796.
- Masuda S, Oda Y, Sasaki H, Ikenouchi J, Higashi T, Akashi M, Nishi E, Furuse M. 2011. LSR defines cell corners for tricellular tight junction formation in epithelial cells. *J Cell Sci.* 124(Pt 4):548–555.
- Mei M, Xiang RL, Cong X, Zhang Y, Li J, Yi X, Park K, Han JY, Wu LL, Yu GY. 2015. Claudin-3 is required for modulation of paracellular permeability by TNF- α through ERK1/2/slug signaling axis in submandibular gland. *Cell Signal.* 27(10):1915–1927.
- Morampudi V, Graef FA, Stahl M, Dalwadi U, Conlin VS, Huang T, Vallance BA, Yu HB, Jacobson K. 2017. Tricellular tight junction protein tricellulin is targeted by the enteropathogenic *Escherichia coli* effector EspG1, leading to epithelial barrier disruption. *Infect Immun.* 85(1):e00700-16.
- Morozko EL, Nishio A, Ingham NJ, Chandra R, Fitzgerald T, Martelletti E, Borck G, Wilson E, Riordan GP, Wangemann P, et al. 2015. ILDR1 null mice, a model of human deafness DFNB42, show structural aberrations of tricellular tight junctions and degeneration of auditory hair cells. *Hum Mol Genet.* 24(3):609–624.
- Nayak G, Lee SI, Yousaf R, Edelmann SE, Trincot C, Van Itallie CM, Sinha GP, Rafeeq M, Jones SM, Belyantseva IA, et al. 2013. Tricellulin deficiency affects tight junction architecture and cochlear hair cells. *J Clin Invest.* 123(9):4036–4049.
- Raleigh DR, Marchiando AM, Zhang Y, Shen L, Sasaki H, Wang Y, Long M, Turner JR. 2010. Tight junction-associated MARVEL proteins marvelD3, tricellulin, and occludin have distinct but overlapping functions. *Mol Biol Cell.* 21(7):1200–1213.
- Riazuddin S, Ahmed ZM, Fanning AS, Lagziel A, Kitajiri S, Ramzan K, Khan SN, Chattaraj P, Friedman PL, Anderson JM, et al. 2006. Tricellulin is a tight-junction protein necessary for hearing. *Am J Hum Genet.* 79(6):1040–1051.
- Sang Q, Li W, Xu Y, Qu R, Xu Z, Feng R, Jin L, He L, Li H, Wang L. 2015. ILDR1 deficiency causes degeneration of cochlear outer hair cells and disrupts the structure of the organ of Corti: a mouse model for human DFNB42. *Biol Open.* 4(4):411–418.
- Stahelin LA, Mukherjee TM, Williams AW. 1969. Freeze-etch appearance of the tight junctions in the epithelium of small and large intestine of mice. *Protoplasma.* 67(2):165–184.
- Tsukita S, Furuse M, Itoh M. 2001. Multifunctional strands in tight junctions. *Nat Rev Mol Cell Biol.* 2(4):285–293.
- Walker DC, MacKenzie A, Hulbert WC, Hogg JC. 1985. A re-assessment of the tricellular region of epithelial cell tight junctions in trachea of guinea pig. *Acta Anat (Basel).* 122(1):35–38.
- Yamaki T, Ohtake K, Ichikawa K, Uchida M, Uchida H, Oshima S, Juni K, Kobayashi J, Morimoto Y, Natsume H. 2013. Poly-L-arginine-induced internalization of tight junction proteins increases the paracellular permeability of the Caco-2 cell monolayer to hydrophilic macromolecules. *Biol Pharm Bull.* 36(3):432–441.
- Zhang LW, Cong X, Zhang Y, Wei T, Su YC, Serrão AC, Brito AR Jr, Yu GY, Hua H, Wu LL. 2016. Interleukin-17 impairs salivary tight junction integrity in Sjögren’s syndrome. *J Dent Res.* 95(7):784–792.